Conservation of Lipid Functions in Cytochrome *bc* Complexes

S. Saif Hasan[1], **Eiki Yamashita**[2], **Christopher M. Ryan**[3], **Julian P. Whitelegge**[3], and **William A. Cramer**[1]

[1]Department of Biological Sciences, Purdue University, West Lafayette IN 47907, USA

[2]Institute of Protein Research, Osaka University, Osaka, Japan

[3]Pasarow Mass Spectrometry Laboratory, NPI-Semel Institute, UCLA, Los Angeles CA, USA

Abstract

Lipid binding sites and properties are compared in two families of hetero-oligomeric membrane protein complexes known to have similar functions in order to gain further understanding of the role of lipid in the function, dynamics, and assembly of these complexes. Using the crystal structure information for both complexes, lipid binding properties were compared for the cytochrome b_6f and bc_1 complexes that function in photosynthetic and respiratory membrane energy transduction. Comparison of lipid and detergent binding sites in the b_6f complex with those in bc_1 shows significant conservation of lipid positions. Seven lipid binding sites in the cyanobacterial b_6f complex overlap three natural sites in the *C. reinhardtii* algal complex, and four sites in the yeast mitochondrial bc_1 complex. The specific identity of lipids is different in b_6f and bc_1 complexes: b_6f contains SDG, PG, MGDG, and DGDG, whereas cardiolipin, PE, and PA are present in the yeast bc_1 complex. The lipidic chlorophyll *a* and *β*-carotene in cyanobacterial b_6f, as well as eicosane in *C. reinhardtii*, are unique to the photosynthetic b_6f complex. The inferences of lipid binding sites and functions were supported by sequence, intermolecular distance, and B-factor information on interacting lipid groups and coordinating amino acid residues. The lipid functions inferred in the b_6f complex are: (**i**) substitution of a trans-membrane helix (TMH) by a lipid and chlorin ring; (**ii**) lipid and *β*-carotene connection of peripheral and core domains; (**iii**) stabilization of iron-sulfur protein TMH; (**iv**) n-side charge and polarity compensation; (**v**) *β*-carotene-mediated super-complex with photosystem I complex.

Introduction

The crystal structure of 220 kDa dimeric cytochrome b_6f complex, one of three hetero-oligomeric membrane protein complexes that constitute the electron transport chain of oxygenic photosynthesis, has been determined for the cyanobacteria *M. laminosus* and *Nostoc* PCC 7120 (1–4) and the green alga, *C. reinhardtii* (5). The arrangement of the eight polypeptide subunits and location of the seven prosthetic groups seen the cyanobacterial complex are shown, emphasizing the prosthetic groups (Fig. 1A) and lipids (Figs. 1B, C), in views parallel (Figs. 1A, B; ribbon format) and orthogonal (Fig. 1C; stick format) to the membrane plane.

The b_6f complex contains eight bound prosthetic groups, of which five, four hemes and the [2Fe-2S] cluster, carry out the redox function. Four of the five redox prosthetic groups, with the exception of the heme c_n (6) have corresponding groups in the bc_1 complex (7, 8, 6, 9, 10). A bound chlorophyll a, β-carotene (1, 5), and eicosane (5) are the additional three prosthetic groups in the b_6f complex. The complex can be divided into core and peripheral domains (Fig. 1C). The core of the cytochrome b_6f complex of oxygenic photosynthesis consists of: (**i**) the four TMH cytochrome b subunit containing two trans-membrane hemes, which is structurally and functionally equivalent to the N-terminal TMH (A–D) heme binding domain of the eight TMH cyt b subunit in the bc_1 complex (11–20); (**ii**) subunit IV with three TMH that is structurally homologous to TMH E-G of the bc_1 complex. The peripheral domain of the b_6f complex consists of six single TMH subunits, cytochrome f (21), the Rieske iron-sulfur protein (22), and the small Pet subunits G, N, L, and M that have been described as "hydrophobic sticks" (23).

Previous studies of the b_6f complex have focused mostly on the properties of the protein subunits and their role in carrying out the function. Because the prevalence of internal lipid is now well documented in many integral membrane proteins, it is clear that an understanding of lipid architecture in membrane proteins will be essential for an understanding of function and dynamics, as well as of assembly which must account for insertion and folding not only of trans-membrane helices but also of the interstitial lipid. Furthermore, in the case of electron transfer proteins such as the b_6f complex, the contribution of lipid to the protein structure is relevant in the calculation of relevant dielectric constants and electron transfer pathways.

An essential role of phospholipids in the reconstitution of the activity of membrane proteins has long been known in membrane protein biochemistry (e. g., (24)). However, early reconstitution studies were usually carried out with crude lipid (e.g., soybean, egg phosphatidylcholine), which inevitably provided little information on specific sites of lipid interaction and understanding of the functions of internal lipids in integral membrane proteins. A dependence of crystal structure on the presence of specific lipids has been demonstrated for a number of membrane proteins and protein complexes. These include the photosynthetic lIght-harvesting chlorophyll protein (25), bacteriorhodopsin (26), α-hemolysin heptamer (27), aquaporin (28), GPCR (29, 30), and potassium ion channels (31–33). The membrane proteins with the largest number of distinct lipids and inferred lipid functions are the hetero-oligomeric photosynthetic reaction centers and the electron transport complexes from photosynthetic and respiratory membranes: the bacterial photosynthetic reaction center (34–38), photosynthetic reaction centers II (39–41) and I (42, 40), bovine (43) and bacterial cytochrome oxidase (44, 45), and the cytochrome bc_1 complex (46).

A comparison of the lipid positions, structures, and apparent functions in two or more protein complexes with similar proteins is a useful approach to an understanding of lipid functions in that family of proteins. The extensive similarity of electron transfer and proton translocation function of b_6f and bc_1 complexes has been considered from a structure perspective (47). Conservation between b_6f and bc_1 complexes ("**bc**" or "**ISPbc**" (48) complexes) of the protein core structure was initially demonstrated by similarity/identity of sequence and hydropathy (49, 50), and later confirmed by crystal structures (11–20). Cα RMSD values of superposed cytochrome bc complex structures are summarized (Table 1), along with an alignment of the amino acid sequences of the eight cyt b_6f subunits (Supplementary Material, File A1).

The present study documents the conservation of binding sites of the lipids and lipid-like molecules in cytochrome bc complexes, and uses this conservation and the protein

environment to infer lipid functions. Aspects of lipid structure-function in other hetero-oligomeric cytochrome complexes (the cytochrome oxidases) have been reviewed (44, 45) and the utility of detergent binding sites as markers for native lipids noted (44).

Comparing the bc_1 complex whose core structure and function are closely related to the b_6f complex, eleven phospholipid molecules in the 1.9 Å yeast complex (PDB ID 3CX5) are present in the yeast bc_1 dimeric complex (Supplementary material, Table S1, (20)). One dianionic cardiolipin is shared between the two monomers at the n-side of the dimer interface. A cardiolipin on the n-side periphery of each subunit of the dimer is proposed to function as an anionic antenna for proton uptake and the start of the pathway to the n-side bound semiquinone or quinone (51, 52). Additional lipids in the yeast complex are (per dimer): 4 phosphatidyl-ethanolamines (PE) and 4 phosphatidic acids (PA). Structure analysis of the lipids in cytochrome bc_1 complexes has been complemented by studies of lipid-dependent enzyme activity (53–55).

RESULTS

Conservation of Lipid Binding Sites in Cytochrome bc Complexes

Four sites in the b_6f complex occupied by lipids or detergent molecules overlap four of the six lipid binding sites in the yeast respiratory bc_1 complex (Supplementary material, Table S1). The two sites in bc_1 occupied by phosphatidyl-ethanolamine (PE) are excepted. The lipid data have been obtained by comparison of three cytochrome b_6f structures (PDB ID 1Q90 (5), 2E74 (3), 2ZT9 (4)) with a structure of yeast cytochrome bc_1 complex (PDB ID 3CX5 (20)). Inferences of physiological relevance in binding sites are based on the proximity (≤ 4.0 Å) of reactive amino acid and lipid groups, documented for the seven bound lipids or detergents bound in the cyanobacterial complex (UDM$_p$, DOPC$_p$, DOPC$_n$, SQD, UDM$_{n1}$, UDM$_{n2}$, and UDM$_{n3}$; Supplementary material, Table S2a–g).

Detergents as Markers of LIpid Binding Sites

There is substantial precedent for ordered detergent molecules in integral membrane proteins serving as reliable markers for lipid binding sites (56). There is a total of eight lipid binding sites per monomer in the cyanobacterial and algal b_6f complex, defined by the presence of natural lipids, the detergent used for purification and crystallization, and the synthetic lipids used for crystallization. In addition to native SQD lipid, two sites In the *M. laminosus* cyanobacterial complex are occupied by dioleoyl-phosphatidylcholine (DOPC) lipid (1, 57), and four sites by the non-ionic UDM detergent (Figs. 1B, C), all presumably having displaced the lipid endogenous to that site. The physiological lipids that occupy these sites include SDG, PG, MGDG and DGDG, as shown by mass spectroscopic analysis of the b_6f complex purified from spinach (Fig. 1D). Three native lipid molecules per monomer, 1 SQD and 2 MGDG, have been resolved in the algal complex, in addition to one chlorophyll *a*, *β*-carotene, and eicosane.

Specific Lipid Functions

1. Substitution of a trans-membrane helix of the cytochrome b subunit by a lipid and the *Chl-a* (Fig. 2)

The cytochrome *b* subunit of the bc_1 complex, with eight TMH, shares critical sequence and extensive hydrophobic segment homology with the cytochrome b_6 subunit and subunit IV of the b_6f complex (50), which consist of four and three trans-membrane helices, respectively (1, 5, 3, 4). The C-terminal eighth (H) helix of the cyt *b* (bc_1) complex, missing in the b_6f complex, is located close to the interface of the F- and G-helices, within an interaction distance < 4.0 Å between residues of the H-helix and those of the F/G helix. Superposition

of the crystal structure of the yeast mitochondrial bc_1 (PDB ID 3CX5; (20)) with that of the b_6f complex from cyanobacteria (PDB ID 2E74, 2ZT9) reveals an unprecedented lipid function, i.e., occupation by the lipid molecule DOPC ("DOPC$_n$") of most of the niche between the F- and G- helices of subunit IV (Fig. 2). One of the acyl tails (yellow) of the DOPC$_n$ molecule is inserted in the inter-helix space between the F, G-helices (pink) of subIV, in close contact with the chlorin ring of the chl-a molecule. As noted previously (1, 5, 58), the chlorin ring of the bound chlorophyll a (axially ligated by two H_2O (3) not shown) is inserted between the F and G TMH of subunit IV and occludes most of the central domain of the membrane bilayer that is spanned by the H helix of the cyt b subunit in the bc_1 complex. Thus, a lipid (e. g., DOPC) and a lipid-like molecule (e. g. chl-a) provide the intra- membrane space-filling function of the bc_1 trans-membrane H helix. In the cyanobacterial and algal structures, chl-a contributes to the structure of the Q_p (lumenal) site of plastoquinol oxidation by stabilizing the separation between the F- and G-helices to accommodate the p-side ef-loop, which includes the PEWY (Pro-Glu-Trp-Tyr) sequence (50) that mediates p-side proton transfer from the bound protonated semiquinone (59, 60). A similar function and structural motif around the Q_p site, discussed for the bacterial bc_1 complex (61), is seen in the yeast mitochondrial bc_1 complex (20). The substitution of a lipid and the chlorin ring to fill the space left by the missing H helix implies that in this case the membrane protein abhors a cavity. Studies on the bacterial reaction center indicate, however, provides an example for toleration of the empty space when the cavity results from a missing prosthetic group (62). These observations raise the question as to which structure in bc complexes centered around the F-G helices, that of the b_6f or the bc_1 complex, took precedence in evolution. Analysis of ribosomal-RNA based phylogenetic relationships between proteobacteria, cyanobacteria, firmicutes and members of Chlorobiaceae demonstrates that the 8 TMH respiratory cyt b subunit gene evolved first and gave rise to the 7 TMH cyt b gene, from which the photosynthetic cyt b_6 (4 TMH)/subIV (3 TMH) split genes were derived (48). Therefore, the cyt b_6f complex of oxygenic photosynthesis utilizes a lipid and a chl-a molecule to replace a lost helix in the trans-membrane domain.

2. Connection of small peripheral subunits of b_6f complex to the core (Fig. 3)

The spatial distribution of the subunit polypeptides and their B-factors in the cyanobacterial b_6f complex (Table 2) implies that the b_6f complex has a two-layered structure: (**i**) A relatively stable core that consists of the cyt b_6 subunit, which has the lowest B-factors (45 $Å^2$, Table 2) of all subunits in the complex, and subunit IV, which are the only polytopic polypeptides in the b_6f complex; (**ii**) a peripheral layer consisting of the single TMH of six subunits, the small Pet G, L, M, and N, whose B-factors (Table 2) are substantially larger (57 – 81 $Å^2$) than those of the b_6f – subIV core, together with cyt f and the ISP.

Because the binding site of the p-side lipids consists of residues from cyt b_6 and subunit IV of the core and the single trans-membrane subunits (Supplementary material, Table S2a–b), the p-side lipids function as anchors that bridge the connection between the stable core and the peripheral layer and thereby stabilize the complex. A synthetic DOPC molecule labeled DOPC$_p$ (orange, Fig. 3) is found on the p-side of the cyanobacterial cyt b_6f complex (PDB ID 2E74 and 2ZT9) in a site analogous to a natural galactolipid MGDG$_1$ (Fig. 3, green) in the $C. reinhardtii$ b_6f structure (PDB ID 1Q90) (40). A closer inspection of the DOPC$_p$ binding site (Supplementary material, Table S2b) in the cyanobacterial b_6f complex (PDB ID 2E74) reveals that Pet L, M and N contribute several residues to the binding site and the acyl tails of the lipid have significant interactions with the trans-membrane helices of the Pet L, M and N subunits (Supplementary material, Table S2b). However, Pet G does not interact significantly with DOPC$_p$ in the cyanobacterial complex or MGDG$_1$ in the homologous site in the algal complex (PDB ID 1Q90). It is suggested that the absence of major sequence

conservation between Pet L, M, and N is a consequence of strong interactions with the p-side lipid, which allows a flexibility to adapt to variations in protein sequence.

Role of the β-carotene molecule (Figs. 1B, 1C, 3, 4)—A β– carotene (β-car) pigment molecule, which is separated by 14 Å from the Chl a (1, 5), is inserted into the trans-membrane helical domain of the b_6f complex (Figs. 1B, 1C, 3). The β-car molecule is ~25 Å long, of which a 17 Å segment is embedded in the protein matrix while the rest is exposed to the hydrophobic lipid bilayer. An analysis of the structure of the amino acid residues that constitute the β-car binding site indicates that the protein-embedded 17 Å portion of the β-car acts as an anchor that contributes to the stability of the b_6f monomer. The β-car molecule lies at the interface between the two sub-domains of the b_6f complex (Fig. 4), "core" and "peripheral" discussed later (**Discussions, section 4**), and stabilizes their interactions by forming associations with the subunits from both sub-domains (Supplementary material, Table S3). Pet G, which shows the highest degree of sequence conservation amongst the four small peripheral Pet subunits (73% between cyanobacteria and higher plants, (63)) is proposed to perform a special function as a mediator of interactions between the two sub-domains (see **Discussion**, **sections 4 and 5**). A role for the 8 Å lipid-exposed portion of the β-car molecule in super-complex formation with Photosystem-I is discussed below (**Results, section 5**).

3. Stabilization of the Rieske Iron-Sulfur Protein TMH (Fig. 5)

A phosphatidic acid (PA) in the yeast bc_1 complex (PDB ID 3CX5) is in close association with the *p*-side trans-membrane helical region of the ISP (64–66). It has been proposed that this phospholipid serves as an anchor that stabilizes the ISP TMH as its soluble domain undergoes the large scale motion that enables electron transfer from the p-side bound ubiquinol via the soluble domain of the ISP to the cyt c_1 heme (46). Superposition of the cyanobacterial (PDB ID 2E74, (3)) and algal (PDB ID 1Q90 (5)) b_6f structures with the bc_1 structure (PDB ID 3CX5) reveals the presence of a similar niche in the b_6f complex (Fig. 5). The electron density observed in the ISP-cyt *f* inter-helix region of the cyanobacterial structure has been modeled as a UDM detergent molecule (white/red), while the algal cyt b_6f structure has an eicosane molecule (green) in the same position. Details of the ligand interactions at this site differ between the bc_1 and b_6f complexes. While the polar head-group of the PA lipid permits cross-linking interactions with hydrophilic residues, including Lys272 of the cyt c_1 TMH and Ser73 of the ISP TMH, the interactions mediated by the eicosane molecule in the algal cyt b_6f complex, and UDM$_p$ in the cyanobacterial complex, are restricted to residues that allow van der Waals interactions (Supplementary material, Table S2a). The hydrophobic, 11- carbon tail of the UDM molecule is inserted in the groove formed by the TMH of cyt *f* and ISP and interacts closely with residues in the B- and E-TMH from the cyt b_6 and subIV subunits, respectively

4. Charge and polarity compensation (Figs. 6A, 6B)

As previously discussed in the context of the *C. reinhardtii* structure (67), a charged anionic sulfoquinovosyl-diacylglycerol molecule (SQD) is inserted between the TMH of ISP (orange) and cyt *f* (yellow) on the n-side of the b_6f complex (Fig. 6A). Superposition of the structures of b_6f (PDB ID 2E74, 1Q90) and bc_1 (PDB ID 3CX5) shows that the SQD molecule in cyt b_6f has a corresponding site in the cyt bc_1 complex occupied by another acidic lipid, phosphatidic acid (PA) and a detergent molecule, UDM (Fig. 6B). Mutation of ISP residue N17 that interacts with the SQD head group results in decreased synthesis of cytochrome *f* in *C. reinhardtii* (67). Lys275 of cyt *f* has also been shown to be critical to the stability of the complex (68), presumably because the anionic sulfolipid compensates the positive charge of Lys275. However, in contrast to the b_6f complex, the protein environment around the lipid binding sites in the bc_1 complex does not involve any charge neutralization

interaction between a lipid and a basic residue. The hydrogen bonding potential of amino acid residues is satisfied by PA-protein interaction.

5. Super-complex of the b_6f and photosystem I complexes (Figs. 3, 7)

Based on the location of the β–carotene molecule in the b_6f complex at the protein-lipid interface on the periphery of the complex (69, 5, 3, 70), it was hypothesized that the β–carotene may be involved in formation of a super-complex with other membrane protein complexes of the electron transfer chain, such as photosystem I, which is the terminal complex in the chain (5). A functional super-complex, with stoichiometric amounts of the b_6f and photosystem I complexes, has been isolated from *C. reinhardtii* (71). Further support for this hypothesis is provided by superposition of the b_6f and bc_1 structures. This shows an overlap of the β–carotene (yellow) and the peripheral cardiolipin (green-red) of the bc_1 complex (Fig. 7), which has been implicated in the formation of a super-complex with the cytochrome *c* oxidase (55). Mutagenesis of the cardiolipin binding site that is expected to disrupt the cyt bc_1-cardiolipin interaction leads to decreased stability of the cyt bc_1-cyt *c* oxidase super-complex in yeast mitochondrial membranes (55). EM-tomographic reconstruction of the super-complex particles has confirmed the architecture of the bc_1-oxidase super-complex (72). The peripheral association of cytochrome *c* oxidase with the bc_1 complex leaves the inter-monomer cavity of bc_1 open to the bilayer, which may facilitate exchange of ubiquinone/quinol. Similarly, the formation of a b_6f-PSI super-complex would permit plastoquinone exchange with the bilayer and/or PSII via the open inter-monomer cavity. Analysis of the crystal structures of the b_6f complex from cyanobacteria (PDB ID 2E74, 2ZT9) and *C. reinhardtii* (PDB ID 1Q90) shows that the peripheral region of the complex, which is exposed to the lipid bilayer and contains the β–carotene, also has two additional lipid binding sites occupied by $MGDG_1/DOPC_p$ and $MGDG_2$ within the Pet M/Pet G subunits (Fig. 3).

Discussion

1. n-side H^+ antenna function ("catalytic role" of lipid) (Fig. 8)

An additional lipid-based function, an n-side proton antenna, is proposed, based to a large extent on analogy with the bc_1 complex. In the yeast bc_1 complex, a peripheral anionic cardiolipin has been proposed to serve as an antenna that recruits protons to the n-side bound ubiquinone (51, 52). Lys228, Asp229 of the cyt *b* subunit and several water molecules (H_2O set 31, 141, 257 and 415) could mediate proton transfer to the n-site ubiquinone. An n-side bound plastoquinone is required for analogous function in the b_6f complex. The quinone analog inhibitors, TDS and NQNO, have been observed in the position of a ligand to the heme c_n in a crystal structure of the cyanobacterial b_6f complex (3). An analysis of the b_6f complex does not reveal any analogous acidic lipids or proton conducting residues that lead to the Q_n site (73) and the proton transfer pathway to the inferred plastoquinone binding site is not known. The second cardiolipin in the bc_1 complex (PDB ID 3CX5), located at the n-side surface of the inter-monomer cavity near the lipid-water interface (66), shared by the two monomers of the bc_1 complex, suggests an additional pathway for n-side H^+ uptake in the b_6f complex. Superposition of structures of b_6f and bc_1 complexes shows that two UDM detergent molecules related by a 2-fold symmetry axis perpendicular to the membrane bilayer, occupy a niche in the b_6f complex similar to that of cardiolipin in bc_1 (Fig. 8). The acidic lipid, PG, one of the few acidic lipids in the thylakoid membrane (74–76), located mainly in the *n*-side of the bilayer, has been identified in the b_6f complex (Fig. 1D). Negative ion mass spectrometry demonstrated the presence of approximately stoichiometric amounts of acidic lipids, PG and SL (Fig. 1D). From the overlap in the *n*-side inter-monomer junction of UDM in the b_6f complex with the cardiolipin in bc_1, it is proposed that

PG is the physiological occupant of this site, functioning as an H^+ antenna, similar to the function proposed for cardiolipin in the bc_1 complex (46).

2. Role of Lipid in Structure Stabilization of Hetero-oligomeric Membrane Proteins

In addition to the n-side anchor provided by anionic lipids (sulfolipid in b_6f and PA in bc_1), it is proposed that stabilization of the ISP trans-membrane helix through an "anchor function" reflects a lipid function in bc complexes that restricts motion of TMH through occupation of inter-helical gaps (46). On the n-side, the cyt b_6f structure from *M. laminosus* (3) contains three lipid binding sites at the opening of the inter-monomer cavity, close to the lipid-water interface (Fig. 6A). A natural lipid, SQD (a sulfolipid), is coordinated with a residue from the cytochrome *f* and the ISP trans-membrane helices. Two UDM detergent molecules are found nearby, one of them within hydrogen bonding distance of the SQD head group. Interaction between the two UDM molecules is inferred as their polar head-group oxygen atoms are within hydrogen bonding distance (< 4 Å) (Fig. 6A). The lipids mark the opening of the inter-monomer cavity on the n-side of the bilayer. The cavity becomes progressively smaller toward the p-side. An interesting feature of this lipid network is the acyl chain disorder Fig. 6A), indicating an absence of ordered electron density around the acyl tails in this region. It has been previously suggested elsewhere that such disorder allows a pathway for quinone/quinol diffusion and exchange between the lipid bilayer and the inter-monomer cavity for both the b_6f complex (46, 77), and the yeast cyt bc_1 complex (Fig. 6B; (77)).

3. Role of p-side lipids in stabilization of the peripheral "picket fence"

A unique function attributed to lipids in the cytochrome b_6f complex has been identified on the basis of comparison of polypeptide and lipid B-factors (Tables 2, 3) and discussed above (**Results, section 2**). As links to the core of the cytochrome b_6f complex, the p-side lipids $DOPC_p$ and $MGDG_1$ help stabilize the structure of the complex. The trans-membrane niche between the Pet G subunit and G-helix of subunit IV is occupied by another galactolipid molecule, $MGDG_2$, in the algal cytochrome b_6f complex (PDB ID 1Q90, Fig. 3). This second p-side lipid binding site is unoccupied in the cyanobacterial cytochrome b_6f complexes (PDB ID 2E74 and 2ZT9). In contrast to the lipid binding site formed by Pet L, M and N, the architecture of the Pet G/G-helix (subunit IV) lipid binding site consists of close interactions of one acyl tail of the lipid that is embedded into the groove between the Pet G and G-helix while the other tail is exposed to the hydrophobic bilayer. This "open"-architecture makes the lipid molecule occupying this site more accessible for exchange to the membrane bilayer in comparison to the $MGDG_1/DOPC_p$ binding site (Fig. 3). A comparison of the galactolipid B-factors (Supplementary material, Fig. S2) further supports these conclusions as $MGDG_1$ has lower B-factors than $MGDG_2$. This implies that the lipid binding site formed by Pet L, M and N has a greater affinity for a lipid than the site formed by Pet G and the G-helix of subunit IV. Therefore, $DOPC_p$ and $MGDG_1$ mark a lipid binding site that serves as an anchor to link the small peripheral Pet subunits to the core of the complex.

In addition, two of the common galactolipids, monogalactosyldiacyl-glycerol (MGDG) and digalactosyl-diacylglycerol (DGDG) have also been detected in cyt b_6f complex purified from spinach thylakoid membranes (Fig. 1D). The crystal structure of the eukaryotic cytochrome b_6f complex from *C. reinhardtii* was solved in the presence of natural lipids (5). While two galactolipids were detected on the p-side of the complex (PDB ID 1Q90), the moderately high resolution (3.1 Å) did not allow the unequivocal identification of the galactolipids and they were modeled as MGDG. The identification of both species of galactolipids in the eukaryotic b_6f complex indicates that one of the two lipids in the algal cytochrome b_6f complex may be a DGDG molecule.

4. Stabilization of the bi-partite cyt b$_6$f structure by β-car; function of Pet G and Pet N

The structure of the cyt b_6f monomer is divided into two sub-domains- (a) a polytopic sub-domain and (b) a single TMH sub-domain. The former consists of cyt b_6 and subIV that have four and three TMH, respectively while the latter is composed of the single TMH subunits Pet L, M, N, cyt f and ISP (Fig. 4). The β –car pigment molecule forms connections with polypeptides from both sub-domains to provide stabilizing interactions within the trans-membrane domain of the monomer. Along with the β –car pigment molecule that lies at the interface of the two sub-domains for structural stabilization, the Pet G subunit performs a unique function in this bi-partite organization. Pet G mediates contacts between the two sub-domains by interacting extensively with the residues from the polytopic sub-domain and also with amino acid residues from sub-units in the single TMH sub-domain (Supplementary Material, Table S4). Pet N, which has been shown to be critical to the stability of the b_6f complex (78), also borders the interface between the two sub-domains. It interacts with residues from the single TMH sub-domain (Supplementary Material, Table S5) to form a network of interactions between the components of this sub-domain. Its association with the polytopic sub-domain is mediated by its interactions with the β-car molecule (Supplementary Material, Table S3).

The observation that the structure of the cyt b_6f monomer is divided into two distinct sub-domains that interact closely with each other via the β –car molecule and the Pet G and Pet N polypeptides may explain the reason behind the sequence conservation of Pet G and Pet N (Supplementary material, File A1). As these two Pet subunits are form extensive associations that stabilize the monomer, they rely on protein-protein interactions. Large changes in amino acid sequences could disrupt these interactions, leading to loss of structural stability of the cyt b_6f complex. Hence, there is an evolutionary pressure for the conservation of Pet G and N sequences.

It is of significance to note that a PE molecule replaces Pet G in cyt bc_1 (Supplementary material, Fig. S1). Due to the absence of Pet subunits from the mitochondrial cyt bc_1 complex, the exact role of the PE molecule in this niche is not understood.

5. Photosynthetic pigments as analogs of lipids in the cytochrome b$_6$f complex

The presence of the photosynthetic pigments, chlorophyll-a and β-carotene is a unique feature of the b_6f compared to the bc_1 complex. The function of the chlorophyll-a and β –carotene molecules is not obvious as they are not known to have any light-dependent reactions in the complex. It was suggested in early structure studies on the b_6f complex that the Chl-a may have a lipid-like function, and that the large separation (14 Å) of the β –carotene from the Chl-a implied that the β –carotene did not have the sole function of triplet state quenching (79, 1, 80, 23). It has been inferred previously that the Chl-a molecule contributes to the structural integrity of the Q_p site (5). The present study invokes several lipidic functions of the single Chl-a and β –carotene in the b_6f complex. The occupation of the niche between the F- and G-helices of Sub IV by chl-a and $DOPC_n$ creates space on the p-side. The ef-loop, which has the catalytically important PEWY sequence (59), is inserted in this space. Hence, the Chl-a molecule contributes to the formation of the Q_p site. The β –carotene is multi-functional on the level of structure. It functions as an anchor of the small peripheral subunits. Moreover, it lies at the interface of the polytopic and single TMH sub-domains of the cyt b_6f monomer and hence, serves an interface around which the complex is stabilized. Moreover, as part of the β –carotene molecule is exposed to the hydrophobic lipid bilayer, it is proposed to be involved in super-complex formation. The β –carotene has also been proposed to be involved in early steps of assembly of the cyt b_6f complex (81, 23).

A lipid-like eicosane molecule is found in the p-side trans-membrane niche between the cyt f and ISP TMH in the algal cyt b_6f complex (Fig. 5). This position is occupied by a UDM_p detergent molecule in the cyanobacterial cyt b_6f complex (PDB ID 2E74, 2ZT9). The natural ligand in this position may have been lost from the complex during purification on a hydrophobic propyl-agarose chromatography column. The eicosane and UDM_p molecules serve two purposes. First, the molecules occupy the space between the cyt f and ISP TMH, thereby stabilizing the complex during ISP soluble domain motion during catalysis. In addition, the molecules contact the polytopic core in addition to the cyt f and ISP TMH and hence, add to the stability of the cyt b_6f complex (Supplementary material, Table S2a).

6. Conservation of amino acid ligands to lipids

A list of residues forming the lipid binding sites in the cyanobacterial cyt b_6f complex (PDB ID 2E74) is provided (Supplementary material, Tables S2a–g) and an alignment of the eight cyt b_6f Pet subunit sequences is summarized (Supplementary material, File A1). Cyt f (PetA), cyt b_6 (PetB), ISP (PetC) and SubIV (PetD) show significant sequence conservation, in general. The residues from these polypeptides contributing to the lipid binding sites are also well-conserved in most instances, with a few exceptions (Supplementary material, File A1). Of the four small peripheral Pet subunits, the sequence of Pet G and N shows partial conservation (Supplementary material, File A1). Pet G does not interact with any lipids to a significant extent. Four residues in Pet N contribute to the $DOPC_p$ binding site- Trp8, Leu11, Leu12 and Phe15 (Supplementary material, Tables S2b). The aromatic residues are well conserved while Leu11 and Leu12 are substituted by other amino acids in different organisms. The remaining two peripheral Pet subunits, Pet L and M, are not as highly conserved as Pet G and N. Both Pet L and M contribute residues to the $DOPC_p$ binding site (Supplementary material, Tables S2b) but do not show any conservation of the amino acids except Tyr8 of Pet L, which is semi-conserved (Supplementary material, File A1). In the Pet L subunit of Synechocystis PCC 6803, it is substituted by a phenylalanine residue.

Thus, amino acids that make up lipid binding sites tend to follow the overall trend of sequence conservation of the polypeptide. The four large subunits- cyt f, cyt b_6, ISP and subIV- have a higher degree of sequence conservation than the smaller Pet subunits and their lipid-interacting residues are also more conserved (Supplementary material, Tables S2a–g and File A1).

7. B-factor analysis of lipids, detergents and binding site residues in the cyt b$_6$f complex

A summary of the B-factors of lipid and detergent molecules and their amino acid ligands in cyt b_6f (PDB ID 2E74) is provided in Table 3 and Supplementary material, Tables S2a–g and S6. The synthetic $DOPC_p$ molecule interacts mainly via its acyl tails (average B-factor=77 Å^2) and not its head-group atoms (average B-factor=164 Å^2). This distribution of B-factors reflects the general trend of lipid association on the p-side of the cyt b_6f complex and is also seen in the physiological MGDG molecules in the algal cyt b_6f structure (Supplementary material, Fig. S2). In the case of the other p-side ligand in the cyanobacterial cyt b_6f complex, UDM_p, close association of the carbon tail with trans-membrane helices is deduced from the average B-factor value of 52 Å^2 of the tail, which is significantly lower than the head group average B-factor value of 122 Å^2. In all these cases, the function of the p-side ligand is occupation of a trans-membrane niche to stabilize the structure of the hetero-oligomeric cyt b_6f complex and to provide structural links between single TMH subunits and a polytopic core.

On the n-side, $DOPC_n$, occupies the space between the F- and G-helices of sub IV. One of the acyl tails of the lipid is embedded in the groove formed by the F- and G-helices and is ordered while the other is more distal and disordered. Both the head group and tail atoms

have similar B-factors, which is explained by the close association of the head group and acyl tail of the lipid with the F- and G-helix groove. The only physiological lipid in the cyanobacterial cyt b_6f complex, SQD (sulfolipid), functions as a cross-linker between the TMH of cyt f and ISP. It has a relatively mobile head group (average B-factor=107 Å^2) and completely disordered acyl tails (Fig. 6A, Table 3). Strong interaction of a lipid with the protein environment is evident in relatively low lipid B-factors, such as those observed for the acyl tails of DOPC$_p$ and UDM$_p$. However, unlike the DOPC$_p$ and UDM$_p$ binding sites, which consist of extensive interactions of the acyl tails with TMHs, the binding of SQD has fewer lipid-protein connections (Supplementary material, Table S2d) and, hence, SQD has high mobility. The n-side UDM molecules, UDM$_{n1}$, UDM$_{n2}$ and UDM$_{n3}$, show higher mobility of head-group atoms (Table 3). This could be a consequence of the non-physiological nature of the detergent molecules UDM, whose head-group does not resemble any physiological photosynthetic lipid. The acyl tails have relatively lower B-factors.

The distribution of binding site B-factors is directly related to the subunits that make up the lipid binding site. Cyt b_6 residues tend to lower the binding site B-factor while the small peripheral Pet subunits increase the B-factors of the lipid binding sites (Table 3).

Methods

1. Isolation and Purification of the b$_6$f complex

Isolation of the cytochrome b$_6$f complex from the two cyanobacteria, *M. laminosus* (1, 57, 3) and *Nostoc* PCC 7120 (4) has recently been summarized (82). Because of the difficulty in separating the b_6f complex from the auxiliary pigment-protein complexes, purification required that the detergent-extracted cytochrome complex be separated by passage through a hydrophobic propyl-agarose column (57), which resulted in delipidation. The lipid DOPC was added to the isolated complex (lipid: cyt f molar stoichiometery = 10:1) after the last step (sucrose gradient) in the purification, prior to crystallization. The purification of the spinach cytochrome b_6f complex has also been described (83).

2. Structural superposition of crystal structures of cytochrome b$_6$f and bc$_1$ complexes (Table 1)

Coordinates of cytochrome b_6f complexes (PDB ID 2E74 and 1Q90) and cytochrome bc_1 complexes (PDB ID 3CX5) were obtained from the PDB (84). All structure superpositions were performed in PyMol (http://www.pymol.org). For identification of the substitute for the cyt bc_1 C-terminal eighth helix of the cyt b subunit in cytochrome b_6f complex, the amino acid sequences of cytochrome b (chain C, PDB ID 3CX5) and subunit IV (chain B, PDB ID 2E74) were aligned in ClustalW (85) using default parameters (Supplementary material, File A2). Residues Asn34-Phe160 of subunit IV were found to align with Lys228-Ile354 of cytochrome b without any gaps. A C-α pair-fit alignment was performed between subunit IV of cytochrome b_6f (PDB ID 2E74, Chain B, Asn34-Phe160) and cytochrome b of cytochrome bc (PDB ID 3CX5, Chain C, Lys228-Ile354) to a C-α root mean square deviation (RMSD) of 4.70 Å. For the analysis of conservation of lipid binding sites between the cyanobacterial cytochrome b_6f complex (PDB ID 2E74) and the algal cytochrome b_6f complex (PDB ID 1Q90), all prosthetic groups, lipids, detergents and water molecules were omitted from the structure. The following peptide regions were also removed from the coordinates: 6-histidine tag at the C-terminus of cytochrome f (PDB ID 1Q90, Chain A) introduced for the purification of the complex, entire soluble domain of the Rieske Iron-Sulfur Protein (Chain C, PDB ID 1Q90 and Ser49-Val179 of Chain D, PDB ID 2E74). A global alignment was performed using the "align" command to a C-α RMSD of 0.65 Å. The prosthetic groups, lipids, detergents, water molecules and the soluble domain of the Rieske Iron – Sulfur Protein were re-introduced in the aligned structures for analysis of ligand

conservation. To study the conservation of a ligand (UDM$_p$ molecule in PDB ID 2E74 and an eicosane in PDB ID 1Q90) in the p-side pocket between the trans-membrane helices of the Rieske Iron-Sulfur protein and cytochrome f of the cytochrome b_6f complex, and a phosphatidic acid in a similar niche between the Rieske Iron sulfur protein and cytochrome c_1 trans-membrane helices of cytochrome bc_1, the cyanobacterial and algal cyt b_6f complexes were superposed as described above. The coordinates of cytochrome bc_1 (PDB ID 3CX5) were then superposed on the structure of the cyanobacterial cytochrome b_6f complex using a global alignment (RMSD=1.29 Å).

3. Structural analysis of lipids, lipid analogs and β-carotene (Table 3 and Supplementary material, Table S6)

The structure of cyt b_6f complex from *M. laminosus* (PDB ID 2E74) was analyzed in COOT (86). 2Fo-Fc electron density map was contoured at 1.0 sigma (~0.1 electrons/Å^3). All lipid, lipid analog (detergent) and $β$–carotene atoms outside the electron density envelop were classified as disordered and omitted from further analysis. Average B-factors were obtained for each lipid and detergent molecule using B-factor data for ordered atoms only and are summarized in Table 3.

4. Structural analysis of lipid binding sites (Table 3 and Supplementary material, Table S2a–g)

Amino acid residues forming the binding sites of lipids, detergents and $β$–carotene in cytochrome b_6f (PDB ID 2E74) were obtained from Ligand Protein Contact Server (87). An amino acid-lipid distance cut-off of 4.0 Å was used to omit residues that were too far to contribute to lipid-protein interactions. The crystallographic asymmetric unit of cytochrome b_6f (PDB ID 2E74) contains the b_6f monomer while the biologically functional unit is the dimer. As the Ligand Protein Contact server database utilizes structural information from the Protein Data Bank, several amino acid residues from one cytochrome b_6f monomer that contribute to lipid binding sites in the other monomer are not included in the Ligand Protein Contact server database. Hence, amino acid residues within a distance of 4.0 Å from a lipid/detergent were further identified in PyMol for the dimeric cytochrome b_6f complex (PDB ID 2E74). The coordinates of the dimeric cytochrome b_6f complex (PDB ID 2E74) were also analyzed in COOT. The 2Fo-Fc electron density map was contoured at 1.0 sigma (~0.1 electrons/Å^3) and inter-atomic distances were measured manually for each amino acid-lipid/detergent/$β$-carotene pair. Only ordered atoms of amino acids and lipids/detergents/$β$-carotene were included in the measurement of inter-atomic distances ("ordered atoms" were defined as the atoms within the 2Fo-Fc electron density envelop at a 1.0 sigma contour level). All residues farther than 4.0 Å from their respective lipid/detergent or $β$-carotene were not considered to contribute to the binding site and omitted from the calculation of lipid binding site B-factors.

5. Analysis of sequence conservation

Sequences of cytochrome b_6f subunits were obtained from the NCBI database (accession numbers summarized in Supplementary material, File A1). Sequence alignment was performed in ClustalW using default parameters.

6. Mass Spectroscopy

Cytochrome b_6f complex. 1.2 mg purified from spinach (82) was extracted with chloroform/methanol (88). Positive ion mass spectrum of ammoniated neutral lipids (M+NH$_4$)$^+$ after a reverse-phase separation of a chloroform extract of cytochrome b_6f complex. The 764.4 and 792.6 Da species are assigned as the (M+NH$_4$)$^+$ ions of monogalactosyldiacylglycerol (MGDG) with 16:3, 18:3 and 18:3, 18:3 fatty acids respectively (C$_{43}$H$_{70}$O$_{10}$ and C$_{45}$H$_{74}$O$_{10}$

calculated monoisotopic masses 746.49 & 774.53 Da, for the neutral species). The 926.7 and 954.6 Da species are assigned as the $(M+NH_4)^+$ ions of digalactosyldiacylglycerol (DGDG) with 16:3, 18:3 and 18:3, 18:3 fatty acids respectively ($C_{49}H_{80}O_{15}$ and $C_{51}H_{84}O_{15}$ calculated monoisotopic masses 908.55 & 936.58 Da, for the neutral species). B. The negative-ion mass spectrum (m/z 700 – 870) of the same sample is shown. The 741.6 Da species is assigned as the $(M-H^+)^-$ ion of phosphatidylglycerol (PG) with 16:1 and 18:3 fatty acids ($C_{40}H_{71}O_{10}P_1$; calculated monoisotopic mass 742.48 Da, for the neutral species). The ions at 815.4 and 837.6 Da are assigned as $(M-H^+)^-$ ions of sulfoquinovosyldiacylglycerol (SDG) with either 16:0, 18:3 or 18:3, 18:3 fatty acids respectively ($C_{43}H_{78}O_{12}S_1$ and $C_{45}H_{76}O_{12}S_1$ calculated monoisotopic masses 816.51 & 838.49 Da, for the neutral species).

Supplementary Material

Refer to Web version on PubMed Central for supplementary material.

Acknowledgments

Abbreviations

β-**Car**	beta-carotene
Chl *a*	chlorophyll *a*
cyt	cytochrome
cyt *bc*	cytochrome bc_1 and b_6f complex
DDM	n-dodecyl- β-D-maltopyranoside
DGDG	digalactosyl diacylglycerol
DOPC$_p$ and DOPC$_n$	dioleoylphosphatidyl choline on electrochemically positive and negative sides of cyanobacterial cyt b_6f
GPCR	G-protein coupled receptor
ISP	Rieske [2Fe-2S] iron-sulfur protein
LHC	light-harvesting chlorophyll protein
MGDG$_1$	monogalactosyl diacylglycerol in algal cyt b_6f that overlaps DOPC$_p$ in cyanobacterial cyt b_6f
MGDG$_2$	monogalactosyl diacylglycerol in algal cyt b_6f in vicinity of MGDG$_1$
NQNO	2n-nonyl-4-hydroxy-quinoline-N-oxide
p-	n-sides of membrane, electrochemically positive and negative
PDB	Protein Data Bank
PA	phosphatidic acid

PG	phosphatidyl-glycerol
PSI, PSII	photosynthetic reaction centers I ands II
RMSD	C-α room mean square deviation
SQD	sulfoquinovosyl-diacylglycerol
subIV	subunit IV of the b_6f complex
TMH	trans-membrane helix
TDS	tridecyl-stigmatellin
UDM	n-undecyl-β-D-maltopyranoside

References

1. Kurisu G, Zhang H, Smith JL, Cramer WA. Structure of the cytochrome b_6f complex of oxygenic photosynthesis: tuning the cavity. Science (New York, NY. 2003; 302:1009–1014.

2. Yan J, Kurisu G, Cramer WA. Structure of the cytochrome b_6f complex: Binding site and intraprotein transfer of the quinone analogue inhibitor 2,5-dibromo-3-methyl-6-isopropyl-*p*-benzoquinone. Proc Nat Acad Sci USA. 2006; 103:67–74.

3. Yamashita E, Zhang H, Cramer WA. Structure of the cytochrome b_6f complex: quinone analogue inhibitors as ligands of heme c_n. J Mol Biol. 2007; 370:39–52. [PubMed: 17498743]

4. Baniulis D, Yamashita E, Whitelegge JP, Zatsman AI, Hendrich MP, Hasan SS, Ryan CM, Cramer WA. Structure-Function, Stability, and Chemical Modification of the Cyanobacterial Cytochrome b_6f Complex from Nostoc sp. PCC 7120. J Biol Chem. 2009; 284:9861–9869. [PubMed: 19189962]

5. Stroebel D, Choquet Y, Popot JL, Picot D. An atypical heam in the cytochrome b_6f complex. Nature. 2003; 426:413–418. [PubMed: 14647374]

6. Zatsman AI, Zhang H, Gunderson WA, Cramer WA, Hendrich MP. Heme-heme interactions in the cytochrome b_6f complex: EPR spectroscopy and correlation with structure. J Amer Chem Soc. 2006; 128:14246–14247. [PubMed: 17076484]

7. Lavergne J. Membrane potential-dependent reduction of cytochrome b_6 in an algal mutant lacking photosystem I centers. Biochim Biophys Acta. 1983; 725:25–33.

8. Joliot P, Joliot A. The low-potential electron-transfer chain in the cytochrome *bf* complex. Biochim Biophys Acta. 1988; 933:319–333.

9. Baymann F, Giusti F, Picot D, Nitschke W. The ci/bH moiety in the b_6f complex studied by EPR: a pair of strongly interacting hemes. Proc Nat Acad Sci USA. 2007; 104:519–524. [PubMed: 17202266]

10. Twigg AI, Baniulis D, Cramer WA, Hendrich MP. EPR detection of an O_2 surrogate bound to heme c_n of the cytochrome b_6f complex. J Am Chem Soc. 2009; 131:12536–12537. [PubMed: 19689132]

11. Xia D, Yu CA, Kim H, Xia JZ, Kachurin AM, Yu L, Deisenhofer J. Crystal structure of the cytochrome bc_1 complex from bovine heart mitochondria. Science (New York, NY. 1997; 277:60–66.

12. Iwata S, Lee JW, Okada K, Lee JK, Iwata M, Rasmussen B, Link TA, Ramaswamy S, Jap BK. Complete structure of the 11-subunit bovine mitochondrial cytochrome bc_1 complex. Science (New York, NY. 1998; 281:64–71.

13. Zhang Z, Huang L, Shulmeister VM, Chi YI, Kim KK, Hung LW, Crofts AR, Berry EA, Kim SH. Electron transfer by domain movement in cytochrome bc_1. Nature. 1998; 392:677–684. [PubMed: 9565029]

14. Berry EA, Huang LS, Zhang Z, Kim SH. Structure of the avian mitochondrial cytochrome bc_1 complex. J Bioenerg Biomem. 1999; 31:177–190.

15. Hunte C, Koepke J, Lange C, Rossmanith T, Michel H. Structure at 2.3 Å resolution of the cytochrome bc_1 complex from the yeast *Saccharomyces cerevisiae* with an antibody Fv fragment. Struct Fold Des. 2000; 8:669–684.

16. Gao X, Wen X, Yu C, Esser L, Tsao S, Quinn B, Zhang L, Yu L, Xia D. The crystal structure of mitochondrial cytochrome bc_1 in complex with famoxadone: The role of aromatic-aromatic interaction in inhibition. Biochemistry-Us. 2002; 41:11692–11702.

17. Gao X, Wen X, Esser L, Quinn B, Yu L, Yu C, Xia D. Structural basis for the quinone reduction in the bc_1 complex: A comparative analysis of crystal structure of mitochondrial cytochrome bc_1 with bound substrate and inhibitors at the Qi site. Biochemistry-Us. 2003; 42:9067–9080.

18. Palsdottir H, Lojero CG, Trumpower BL, Hunte C. Structure of the yeast cytochrome bc_1 complex with a hydroxyquinone anion Qo site inhibitor bound. J Biol Chem. 2003; 278:31303–31311. [PubMed: 12782631]

19. Esser L, Quinn B, Li YF, Zhang M, Elberry M, Yu L, Yu CA, Xia D. Crystallographic studies of quinol oxidation site inhibitors: a modified classification of inhibitors for the cytochrome bc_1 complex. J Mol Biol. 2004; 341:281–302. [PubMed: 15312779]

20. Solmaz SR, Hunte C. Structure of complex III with bound cytochrome *c* in reduced state and definition of a minimal core interface for electron transfer. J Biol Chem. 2008; 283:17542–17549. [PubMed: 18390544]

21. Soriano, GM.; Smith, JL.; Cramer, WA. Cytochrome *f*. In: Messerschmidt, A.; Huber, R.; Wieghardt, K.; Poulos, T., editors. Handbook of Metalloproteins. Wiley; London: 2001. p. 172-181.

22. Carrell CJ, Zhang H, Cramer WA, Smith JL. Biological identity and diversity in photosynthesis and respiration: structure of the lumen-side domain of the chloroplast Rieske protein. Structure. 1997; 5:1613–1625. [PubMed: 9438861]

23. Cramer WA, Zhang H, Yan J, Kurisu G, Smith JL. Trans-membrane traffic in the cytochrome b_6f complex. Ann Rev Biochem. 2006; 75:769–790. [PubMed: 16756511]

24. Azzi, A.; Brodbeck, U.; Zahler, P., editors. Membrane Proteins: A Laboratory Manual. Springer-Verlag; Berlin: 1981.

25. Nussberger S, Dorr K, Wang DN, Kuhlbrandt W. Lipid-protein interactions in crystals of the plant light-harvesting complex. J Mol Biol. 1993; 234:347–356. [PubMed: 8230219]

26. Cartailler JP, Luecke H. X-ray crystallographic analysis of lipid-protein interactions in the bacteriorhodopsin purple membrane. Annu Rev Biophys Biomol Struct. 2003; 32:285–310. [PubMed: 12598369]

27. Gantar M, Berry JP, Thomas S, Wang M, Perez R, Rein KS. Allelopathic activity among Cyanobacteria and microalgae isolated from Florida freshwater habitats. FEMS microbiology ecology. 2008; 64:55–64. [PubMed: 18266743]

28. Hite RK, Li ZL, Walz T. Principles of membrane protein interactions with annular lipids deduced from aquaporin-0 2D crystals. Embo Journal. 2010; 29:1652–1658. [PubMed: 20389283]

29. Escriba PV, Wedegaertner PB, Goni FM, Vogler O. Lipid-protein interactions in GPCR-associated signaling. Biochimica et biophysica acta. 2007; 1768:836–852. [PubMed: 17067547]

30. Hanson MA, Cherezov V, Griffith MT, Roth CB, Jaakola VP, Chien EY, Velasquez J, Kuhn P, Stevens RC. A specific cholesterol binding site is established by the 2.8 A structure of the human beta2-adrenergic receptor. Structure. 2008; 16:897–905. [PubMed: 18547522]

31. Lee SY, Lee A, Chen JY, MacKinnon R. Structure of the KvAP voltage-dependent K+ channel and its dependence on the lipid membrane. Proceedings of the National Academy of Sciences of the United States of America. 2005; 102:15441–15446. [PubMed: 16223877]

32. Schmidt D, Cross SR, MacKinnon R. A gating model for the archeal voltage-dependent K(+) channel KvAP in DPhPC and POPE:POPG decane lipid bilayers. J Mol Biol. 2009; 390:902–912. [PubMed: 19481093]

33. Butterwick JA, MacKinnon R. Solution structure and phospholipid interactions of the isolated voltage-sensor domain from KvAP. J Mol Biol. 2010; 403:591–606. [PubMed: 20851706]

34. McAuley KE, Fyfe PK, Ridge JP, Isaacs NW, Cogdell RJ, Jones MR. Structural details of an interaction between cardiolipin and an integral membrane protein. Proceedings of the National

Academy of Sciences of the United States of America. 1999; 96:14706–14711. [PubMed: 10611277]

35. Camara-Artigas A, Brune D, Allen JP. Interaction between lipids and bacterial reaction centers determined by protein crystallography. Proc Nat Acad Sci USA. 2002; 99:11055–11060. [PubMed: 12167672]

36. Fyfe PK, Hughes AV, Heathcote P, Jones MR. Proteins, chlorophylls and lipids: X-ray analysis of a three-way relationship. Trends Plant Sci. 2005; 10:275–282. [PubMed: 15949761]

37. Jones MR. Lipids in photosynthetic reaction centres: structural roles and functional holes. Prog Lipid Res. 2007; 46:56–87. [PubMed: 16963124]

38. Wohri AB, Wahlgren WY, Malmerberg E, Johansson LC, Neutze R, Katona G. Lipidic sponge phase crystal structure of a photosynthetic reaction center reveals lipids on the protein surface. Biochemistry-Us. 2009; 48:9831–9838.

39. Guskov A, Kern J, Gabdulkhakov A, Broser M, Zouni A, Saenger W. Cyanobacterial photosystem II at 2.9-A resolution and the role of quinones, lipids, channels and chloride. Nat Struct Mol Biol. 2009; 16:334–342. [PubMed: 19219048]

40. Kern, J.; Zouni, A.; Guskov, A.; Krauss, N. Lipids in the structure of the photosystem I, photosystem II, and the cytochrome b6f complex. In: Murata, HWaN, editor. Lipids in Photosynthesis: Essential and Regulatory Functions. Springer Science; 2009. p. 203-242.

41. Umena Y, Kawakami K, Shen JR, Kamiya N. Crystal structure of oxygen-evolving photosystem II at a resolution of 1.9 A. Nature. 2011; 473:55–60. [PubMed: 21499260]

42. Jordan P, Fromme P, Witt HT, Klukas O, Saenger W, Krauss N. Three-dimensional structure of cyanobacterial photosystem I at 2.5 A resolution. Nature. 2001; 411:909–917. [PubMed: 11418848]

43. Shinzawa-Itoh K, Aoyama H, Muramoto K, Terada H, Kurauchi T, Tadehara Y, Yamasaki A, Sugimura T, Kurono S, Tsujimoto K, Mizushima T, Yamashita E, Tsukihara T, Yoshikawa S. Structures and physiological roles of 13 integral lipids of bovine heart cytochrome c oxidase. The EMBO journal. 2007; 26:1713–1725. [PubMed: 17332748]

44. Qin L, Hiser C, Mulichak A, Garavito RM, Ferguson-Miller S. Identification of conseved lipid/ detergent binding site in a high resolution structure of the memebrane protein, Cytochrome c oxidase. Proc Natl Acad Sci, USA. 2006; 103:16117–16122. [PubMed: 17050688]

45. Qin L, Sharpe MA, Garavito RM, Ferguson-Miller S. Conserved lipid-binding sites in membrane proteins: a focus on cytochrome c oxidase. Current opinion in structural biology. 2007; 17:444–450. [PubMed: 17719219]

46. Palsdottir H, Hunte C. Lipids in membrane protein structures. Biochim Biophys Acta. 2004; 1666:2–18. [PubMed: 15519305]

47. Cramer WA, Yamashita E, Hasan SS. The Q cycle of cytochrome bc complexes: a structure perspective. Biochim Biophys Acta/Bioenergetics. 2011; 1807:788–802.

48. Schutz M, Brugna M, Lebrun E, Baymann F, Huber R, Stetter KO, Hauska G, Toci R, Lemesle-Meunier D, Tron P, Schmidt C, Nitschke W. Early evolution of cytochrome *bc* complexes. J Mol Biol. 2000; 300:663–675. [PubMed: 10891261]

49. Saraste M. Location of haem-binding sites in the mitochondrial cytochrome *b*. FEBS letters. 1984; 166:367–372. [PubMed: 6363134]

50. Widger WR, Cramer WA, Herrmann RG, Trebst A. Sequence homology and structural similarity between the *b* cytochrome of mitochondrial complex III and the chloroplast b_6f complex: position of the cytochrome *b* hemes in the membrane. Proc Natl Acad Sci, U S A. 1984; 81:674–678. [PubMed: 6322162]

51. Lange C, Nett JH, Trumpower BL, Hunte C. Specific roles of protein-phospholipid interactions in the yeast cytochrome bc1 complex structure. EMBO J. 2001; 20:6591–6600. [PubMed: 11726495]

52. Hunte C, Palsdottir H, Trumpower BL. Protonmotive pathways and mechanisms in the cytochrome bc_1 complex. FEBS letters. 2003; 545:39–46. [PubMed: 12788490]

53. Schagger H, Hagen T, Roth B, Brandt U, Link TA, von Jagow G. Phospholipid specificity of bovine heart bc1 complex. Eur J Biochem. 1990; 190:123–130. [PubMed: 2163831]

54. Wenz T, Covian R, Hellwig P, Macmillan F, Meunier B, Trumpower BL, Hunte C. Mutational analysis of cytochrome *b* at the ubiquinol oxidation site of yeast complex III. J Biol Chem. 2007; 282:3977–3988. [PubMed: 17145759]

55. Wenz T, Hielscher R, Hellwig P, Schagger H, Richers S, Hunte C. Role of phospholipids in respiratory cytochrome bc_1 complex catalysis and supercomplex formation. Biochim Biophys Acta. 2009; 1787:609–616. [PubMed: 19254687]

56. Qin L, Sharpe MA, Garavito RM, Ferguson-Miller S. Conserved lipid-binding sites in membrane proteins: a focus on cytochrome c oxidase. Current Opinion in Structural Biology. 2007; 17:444–450. [PubMed: 17719219]

57. Zhang H, Kurisu G, Smith JL, Cramer WA. A defined protein-detergent-lipid complex for crystallization of integral membrane proteins: The cytochrome b_6f complex of oxygenic photosynthesis. Proc Nat Acad Sci USA. 2003; 100:5160–5163. [PubMed: 12702760]

58. de Lacroix de Lavalette A, Finazzi G, Zito F. b6f-Associated chlorophyll: structural and dynamic contribution to the different cytochrome functions. Biochemistry-Us. 2008; 47:5259–5265.

59. Zito F, Finazzi G, Joliot P, Wollman FA. Glu78, from the conserved PEWY sequence of subunit IV, has a key function in cytochrome b6f turnover. Biochemistry-Us. 1998; 37:10395–10403.

60. Finazzi G. Redox-coupled proton pumping activity in cytochrome b6f, as evidenced by the pH dependence of electron transfer in whole cells of Chlamydomonas reinhardtii. Biochemistry-Us. 2002; 41:7475–7482.

61. Crofts AR, Holland JT, Victoria D, Kolling DR, Dikanov SA, Gilbreth R, Lhee S, Kuras R, Kuras MG. The Q-cycle reviewed: How well does a monomeric mechanism of the bc_1 complex account for the function of a dimeric complex? Biochim Biophys Acta. 2008; 1777:1001–1019. [PubMed: 18501698]

62. Fyfe PK, Potter JA, Cheng J, Williams CM, Watson AJ, Jones MR. Structural responses to cavity-creating mutations in an integral membrane protein. Biochemistry-Us. 2007; 46:10461–10472.

63. Schwenkert S, Legen J, Takami T, Shikanai T, Herrmann RG, Meurer J. Role of the low-molecular-weight subunits PetL, PetG, and PetN in assembly, stability, and dimerization of the cytochrome b6f complex in tobacco. Plant physiology. 2007; 144:1924–1935. [PubMed: 17556510]

64. Lange C, Nett JH, Trumpower BL, Hunte C. Specific roles of protein-phospholipid interactions in the yeast cytochrome bc(1) complex structure. Embo Journal. 2001; 20:6591–6600. [PubMed: 11726495]

65. Hunte C, Richers S. Lipids and membrane protein structures. Current Opinion in Structural Biology. 2008; 18:406–411. [PubMed: 18495472]

66. Solmaz SRN, Hunte C. Structure of complex III with bound cytochrome c in reduced state and definition of a minimal core interface for electron transfer. Journal of Biological Chemistry. 2008; 283:17542–17549. [PubMed: 18390544]

67. de Vitry C, Ouyang Y, Finazzi G, Wollman FA, Kallas T. The chloroplast Rieske iron-sulfur protein. At the crossroad of electron transport and signal transduction. J Biol Chem. 2004; 279:44621–44627. [PubMed: 15316016]

68. Choquet Y, Zito F, Wostrikoff K, Wollman FA. Cytochrome f translation in Chlamydomonas chloroplast is autoregulated by its carboxyl-terminal domain. Plant Cell. 2003; 15:1443–1454. [PubMed: 12782735]

69. Kurisu G, Zhang HM, Smith JL, Cramer WA. Structure of the cytochrome b(6)f complex of oxygenic photosynthesis: Tuning the cavity. Science. 2003; 302:1009–1014. [PubMed: 14526088]

70. Baniulis D, Yamashita E, Whitelegge JP, Zatsman AI, Hendrich MP, Hasan SS, Ryan CM, Cramer WA. Structure-Function, Stability, and Chemical Modification of the Cyanobacterial Cytochrome b(6)f Complex from Nostoc sp PCC 7120. Journal of Biological Chemistry. 2009; 284:9861–9869. [PubMed: 19189962]

71. Iwai M, Takizawa K, Tokutsu R, Okamuro A, Takahashi Y, MInagawa J. Isolation of the supercomplex that drives cyclic electron flow in photosynthesis. Nature. 2010; 464:1210–1213. [PubMed: 20364124]

72. Schafer E, Dencher NA, Vonck J, Parcej DN. Three-dimensional structure of the respiratory chain supercomplex I1III2IV1 from bovine heart mitochondria. Biochemistry-Us. 2007; 46:12579–12585.

73. Cramer, WA.; Baniulis, D.; Yamashita, E.; Zhang, H.; Zatsman, AI.; Hendrich, MP. Structure, spectroscopy, and function of the cytochrome b_6f complex: heme c_n and n-side electron and proton transfer reactions. In: Fromme, P., editor. Photosynthetic Protein Complexes: a Structural Approach. Wiley-VCH; Weinheim: 2008. p. 155-179.

74. Rawyler A, Siegenthaler PA. TRANSMEMBRANE DISTRIBUTION OF PHOSPHOLIPIDS AND THEIR INVOLVEMENT IN ELECTRON-TRANSPORT, AS REVEALED BY PHOSPHOLIPASE-A2 TREATMENT OF SPINACH THYLAKOIDS. Biochimica Et Biophysica Acta. 1981; 635:348–358. [PubMed: 7236668]

75. Unitt MD, Harwood JL. SIDEDNESS STUDIES OF THYLAKOID PHOSPHATIDYLGLYCEROL IN HIGHER-PLANTS. Biochemical Journal. 1985; 228:707–711. [PubMed: 4026805]

76. Gounaris K, Barber J, Harwood JL. THE THYLAKOID MEMBRANES OF HIGHER-PLANT CHLOROPLASTS. Biochemical Journal. 1986; 237:313–326. [PubMed: 3541898]

77. Hunte C. Specific protein-lipid interactions in membrane proteins. Biochem Soc Trans. 2005; 33:938–942. [PubMed: 16246015]

78. Schneider D, Volkmer T, Rogner M. PetG and PetN, but not PetL, are essential subunits of the cytochrome b_6f complex from *Synechocystis* PCC 6803. Research in microbiology. 2007; 158:45–50. [PubMed: 17224258]

79. Kim H, Xia D, Yu CA, Xia JZ, Kachurin AM, Zhang L, Yu L, Deisenhofer J. Inhibitor binding changes domain mobility in the iron-sulfur protein of the mitochondrial bc_1 complex from bovine heart. Proc Natl Acad Sci, U S A. 1998; 95:8026–8033. [PubMed: 9653134]

80. Dashdorj N, Zhang H, Kim H, Yan J, Cramer WA, Savikhin S. The single chlorophyll *a* molecule in the cytochrome b_6f complex: unusual optical properties protect the complex against singlet oxygen. Biophysical journal. 2005; 88:4178–4187. [PubMed: 15778449]

81. Cramer WA, Yan J, Zhang H, Kurisu G, Smith JL. Structure of the cytochrome b_6f complex: new prosthetic groups, Q-space, and the 'hors d'oeuvres hypothesis' for assembly of the complex. Photosynth Res. 2005; 85:133–143. [PubMed: 15977064]

82. Baniulis, D.; Zhang, H.; Yamashita, E.; Zakharova, T.; Hasan, SS.; Cramer, WA. Purification and crystallization of the cyanobacterial cytochrome b6f complex. In: Carpentier, R., editor. Methods in Molecular Biology, Photosynthesis Research Protocols. Humana Press Inc; Totowa, NJ: 2011.

83. Zhang H, Whitelegge JP, Cramer WA. Ferredoxin:NADP$^+$ oxidoreductase is a subunit of the chloroplast cytochrome b_6f complex. J Biol Chem. 2001; 276:38159–38165. [PubMed: 11483610]

84. Bernstein FC, Koetzle TF, Williams GJ, Meyer EF Jr, Brice MD, Rodgers JR, Kennard O, Shimanouchi T, Tasumi M. The Protein Data Bank: a computer-based archival file for macromolecular structures. J Mol Biol. 1977; 112:535–542. [PubMed: 875032]

85. Thompson JD, Higgins DG, Gibson TJ. CLUSTAL W: improving the sensitivity of progressive multiple sequence alignment through sequence weighting, position-specific gap penalties and weight matrix choice. Nucleic Acids Res. 1994; 22:4673–4680. [PubMed: 7984417]

86. Emsley P, Lohkamp B, Scott WG, Cowtan K. Features and development of Coot. Acta Crystallogr D Biol Crystallogr. 2010; 66:486–501. [PubMed: 20383002]

87. Sobolev V, Sorokine A, Prilusky J, Abola EE, Edelman M. Automated analysis of interatomic contacts in proteins. Bioinformatics. 1999; 15:327–332. [PubMed: 10320401]

88. Wessel D, Fluegge U. A method for the quantitative recovery of protein in dilute solution in the presence of detergents and lipids. Anal Biochem Analytical Biochemistry. 1984; 138:141–143.

89. Whitelegge JP, Zhang H, Taylor R, Cramer WA. Full subunit coverage liquid chromatography electrospray-ionization mass spectrometry (LCMS$^+$) of an oligomeric membrane protein complex: the cytochrome b_6f complex from spinach and the cyanobacterium, *M. laminosus*. Mol Cell Prot. 2002; 1:816–827.

90. Dowhan W, Bogdanov M. Lipid-dependent membrane protein topogenesis. Ann Rev Biochemistry. 2006; 78:515–540.
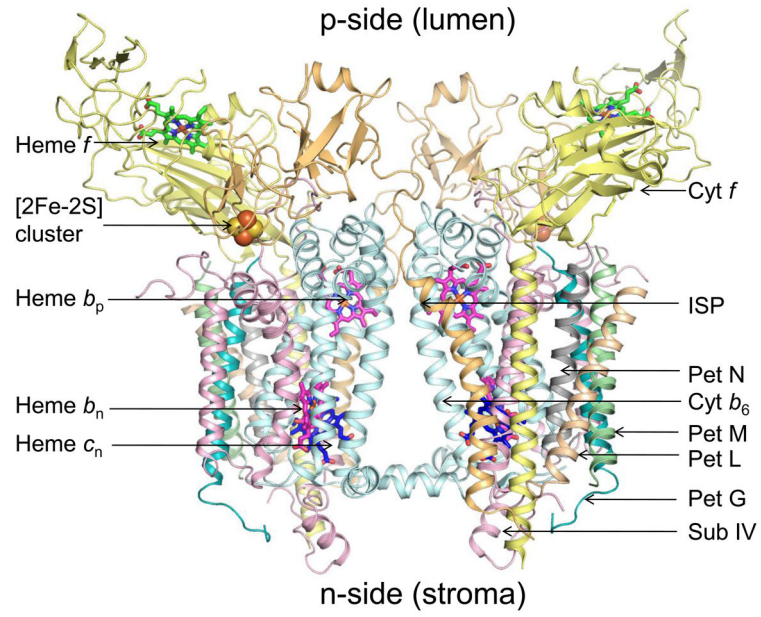
Fig. 1A

Fig. 1B
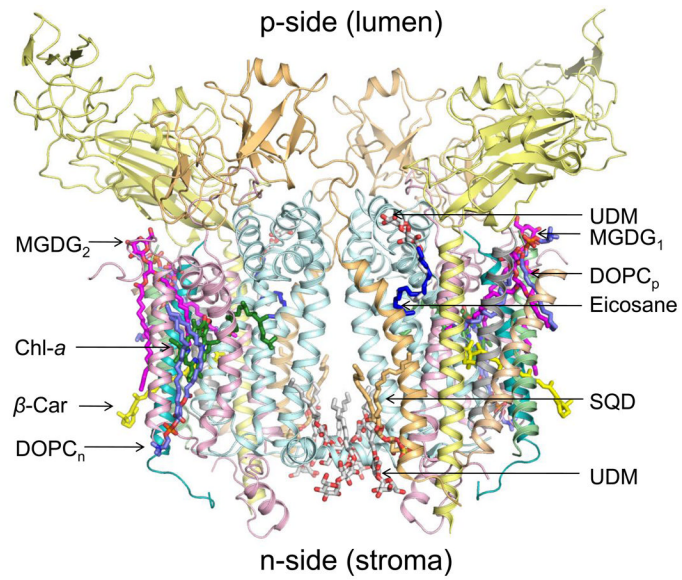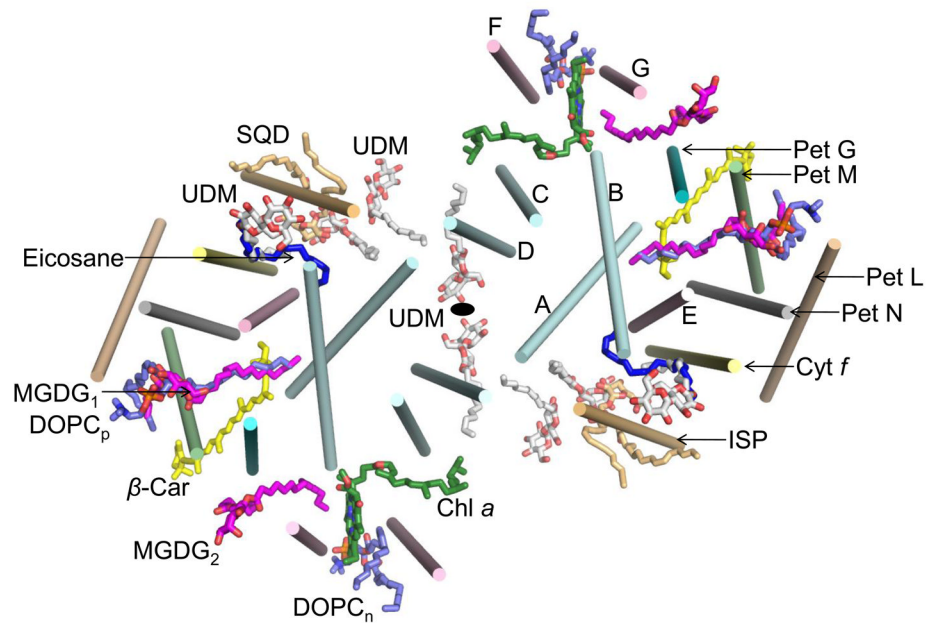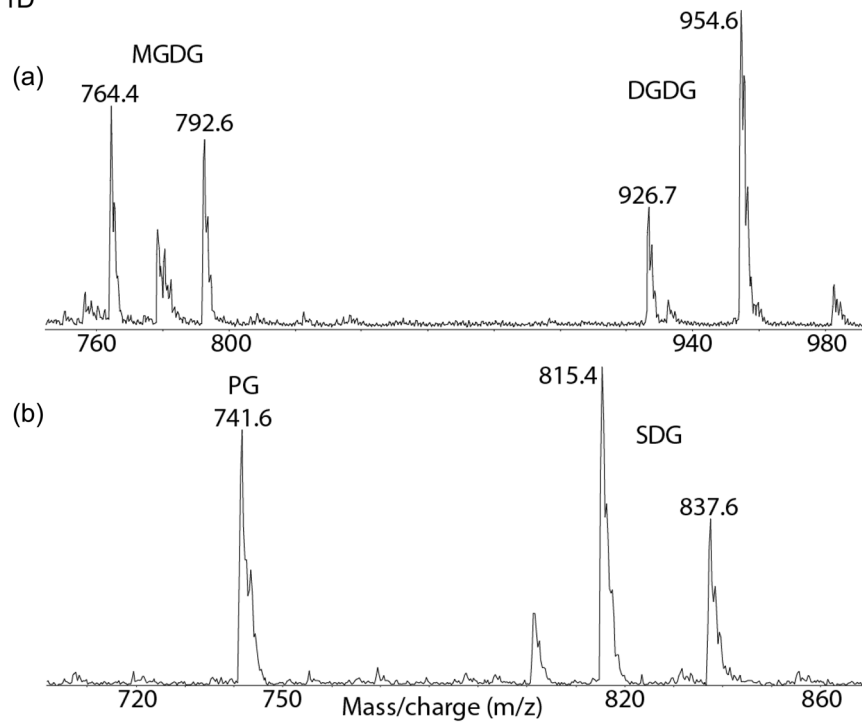
Fig. 1C

Fig. 1D

Fig 1. Subunit organization and lipid binding sites in the cytochrome b_6f complex

(**A**) Dimeric cytochrome b_6f complex from *Mastigocladus laminosus* (PDB ID 2E74), showing the positions of the eight protein subunits. Side view, in plane of membrane. Color code: Cytochrome *f*/Pet A (yellow), cytochrome b_6/Pet B (cyan), Rieske Fe_2S_2 protein/Pet C (orange), subunit IV/Pet D (pink), Pet G (teal), Pet L (light brown), Pet M (green) and Pet N (gray). (**B**) Side view of *M. laminosus* cyt b_6f complex showing lipids, detergents and

pigments. **(C)** Top view along the membrane normal of *M. laminosus* cytochrome b_6f complex (PDB ID 2E74) showing 26 trans-membrane helices and the 2-fold symmetry axis between the monomers. Lipids ($MGDG_1$ and $MGDG_2$, magenta and red) and a pigment (eicosane, blue) from the *C. reinhardtii* b_6f complex were superimposed on the *M. laminosus* b_6f structure by combining PDB ID 2E74 and PDB ID 1Q90. The TMH of cytochrome b_6 (A–D) and subunit IV (E–G), Rieske Iron-Sulfur protein, cytochrome *f*, and the peripheral Pet subunits are shown as cylinders. n, p, electrochemically negative and positive sides of the complex. **(D)** Neutral and anionic lipids in spinach cyt b_6f complex. Major lipids of spinach b_6f complex detected by liquid chromatography with mass spectrometry (89). (**a**). Positive ion mass spectrum of ammoniated neutral lipids $(M+NH_4)^+$ after a reverse-phase separation of a chloroform extract of cytochrome b_6f complex. The 764.4 and 792.6 Da species are assigned as the $(M+NH_4)^+$ ions of monogalactosyldiacylglycerol (MGDG) with 16:3, 18:3 and 18:3, 18:3 fatty acids respectively ($C_{43}H_{70}O_{10}$ and $C_{45}H_{74}O_{10}$ calculated mono-isotopic masses 746.49 & 774.53 Da, for the neutral species). The 926.7 and 954.6 Da species are assigned as the $(M+NH_4)^+$ ions of digalactosyldiacylglycerol (DGDG) with 16:3, 18:3 and 18:3, 18:3 fatty acids respectively ($C_{49}H_{80}O_{15}$ and $C_{51}H_{84}O_{15}$ calculated mono-isotopic masses 908.55 & 936.58 Da, for the neutral species). (**b**). The negative-ion mass spectrum (m/z 700 – 870) of the same sample is shown. The 741.6 Da species is assigned as the $(M\text{-}H^+)^-$ ion of phosphatidylglycerol (PG) with 16:1 and 18:3 fatty acids ($C_{40}H_{71}O_{10}P_1$; calculated mono-isotopic mass 742.48 Da, for the neutral species). The ions at 815.4 and 837.6 Da are assigned as $(M\text{-}H^+)^-$ ions of sulfoquinovosyldiacylglycerol (SDG) with either 16:0, 18:3 or 18:3, 18:3 fatty acids respectively ($C_{43}H_{78}O_{12}S_1$ and $C_{45}H_{76}O_{12}S_1$ calculated mono-isotopic masses 816.51 & 838.49 Da, for the neutral species).
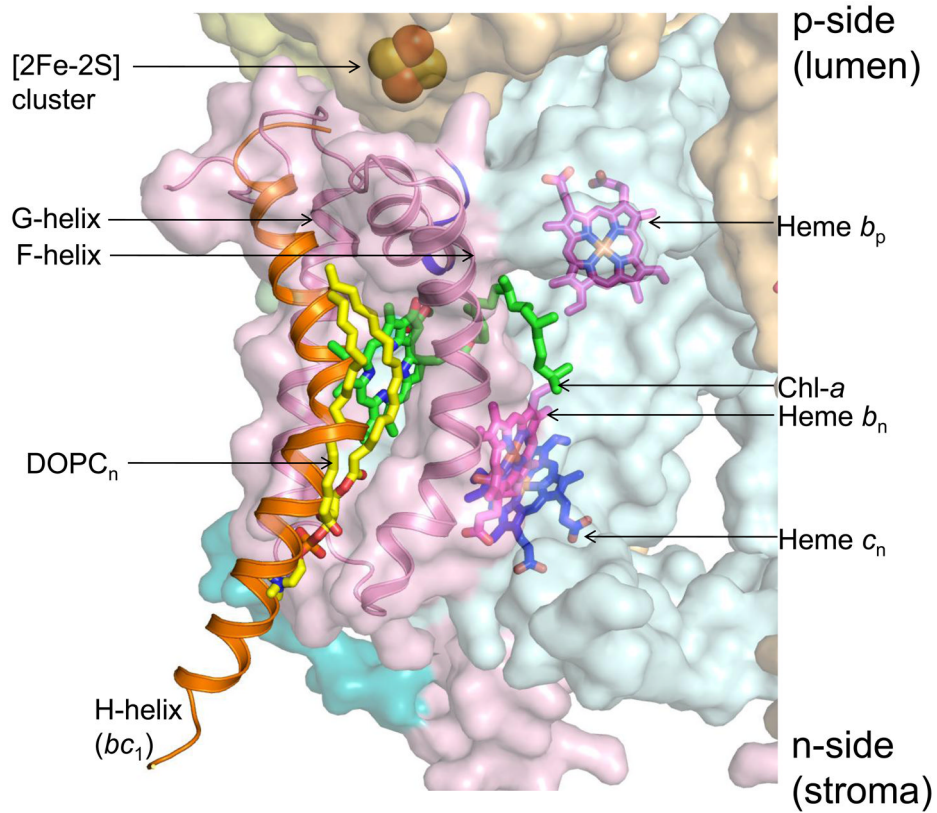
Fig. 2. Substitution of a TMH in bc1 by a lipid and lipid-like chlorophyll a in the b6f complex
C-terminal trans-membrane 8th helix (H-helix, orange) of cyt b subunit of yeast bc_1 complex
(PDB ID 3CX5) interacts with the F- and G-helices. In superimposed b_6f (PDB ID 2E74)
and bc_1 (PDB ID 3CX5) complexes, a DOPC lipid (yellow acyl tails, orange and red head
group), together with the Chl a (green), protrudes from the space between the F- and G-
helices (pink) and fills the niche occupied by the H TMH in the bc_1 complex. Protein chains
of bc_1 subunits not shown.
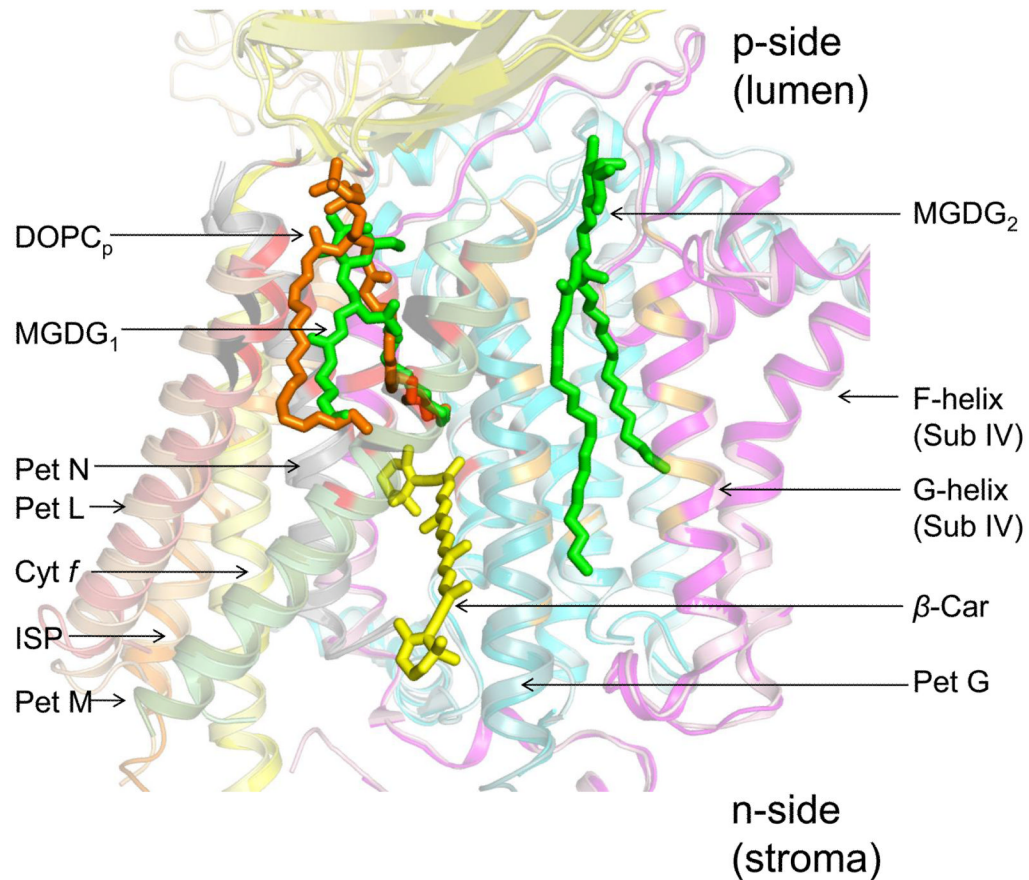
Fig. 3. Lipid-mediated connection of peripheral monotopic Pet G, L, M, and N subunits and the polytopic core of the b_6f complex
The natural galactolipid $MGDG_1$ (green) fills the interstitial space between small Pet G, L, M, and N subunits of the *C. reinhardtii* cyt b_6f complex (PDB ID 1Q90). The artificial lipid $DOPC_p$ (stick format, orange) occupies one of the niches between the small Pet subunits in the cyanobacterial cyt b_6f complex (PDB ID 2E74). Neighboring β – carotene shown in yellow. A second galactolipid, $MGDG_2$, is found inserted between the TMH of Pet G and the G-helix of sub IV of the algal cyt b_6f.
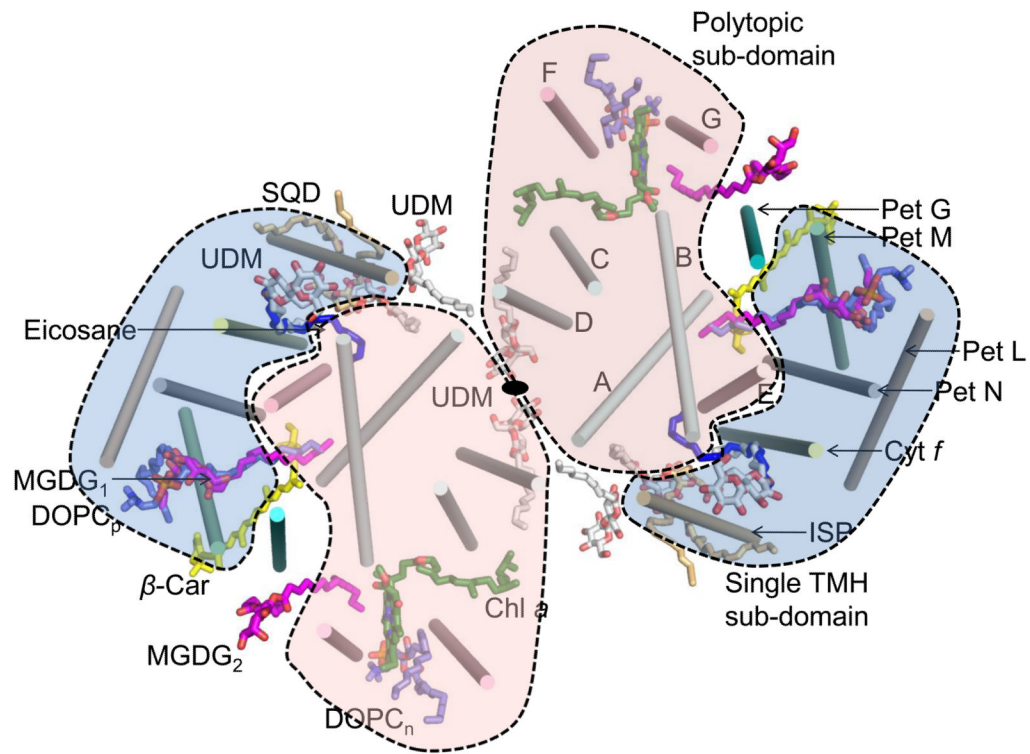
Fig 4. Sub-domain structure of cyt b_6f

The cyt b_6f monomer (PDB ID 2E74) is organized into two distinct sub-domains- (i) a polytopic sub-domain (shown in pink) that consists of cyt b_6 and subIV and constitutes the central portion of the dimer, and (ii) a single TMH sub-domain (shown in blue) that is composed of Pet L, M, N cyt f and ISP. This sub-domain is more peripheral in position. The interface between the two sub-domains is formed by the β–carotene molecule (yellow) and Pet G (teal). View of the cyt b_6f complex along the normal to the membrane (2-fold symmetry axis is shown at the inter-monomer interface).
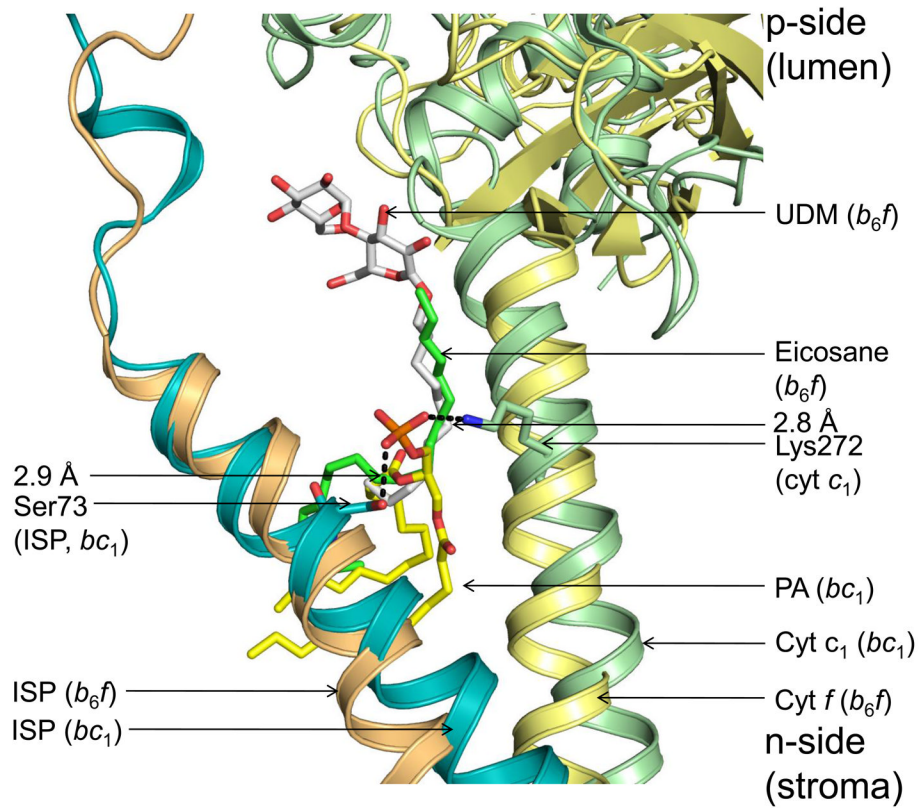
Fig. 5. Acyl chain stabilization of the trans-membrane helix (TMH) of the Rieske iron-sulfur protein (ISP)

The acyl tails of a phosphatidic acid, PA (yellow, orange) of cyt bc_1 is wrapped around the ISP TMH. A UDM (white and red) molecule is located in a similar position in the cyanobacterial b_6f complex, while the niche is occupied by eicosane (green) in the algal b_6f complex. The cyanobacterial (PDB ID 2E74) and algal (PDB ID 1Q90) b_6f complex are superposed with the the yeast bc_1 (PDB ID 3CX5).
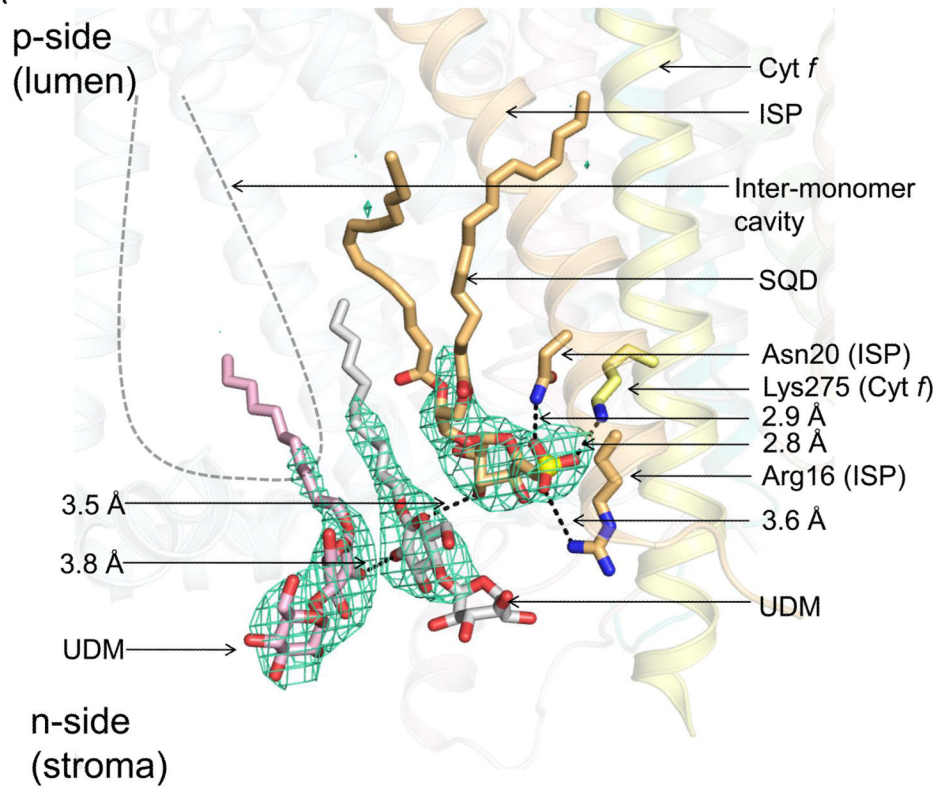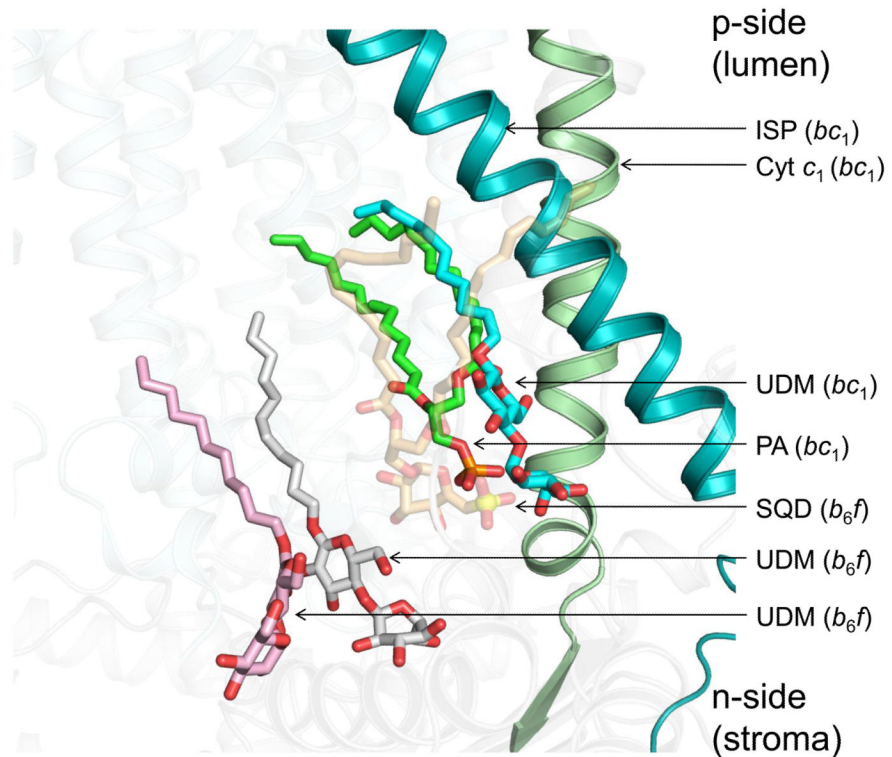
Fig. 6A

Fig. 6B

Fig. 6. n-side charge compensation

Conserved position for binding acidic lipid(s) (46) on the n-side of cyanobacterial b_6f (PDB ID 2E74) and bc_1 complexes (PDB ID 3CX5). **(A)** Three lipid binding sites (1 sulfolipid and 2 UDM molecules) are observed on the n-side of the inter-monomer cavity, close to the lipid-aqueous interface, in each monomer of the cyanobacterial b_6f complex (*M. laminosus* PDB ID 2E74). The head-group of the sulfolipid (color, wheat) is within an interaction distance (3.5 Å) of 1 UDM molecule (white and red), which interacts with another UDM molecule (pink and red, separation 3.8 Å). Disordered acyl chains of sulfolipid and detergent molecules can define a pathway for plastoquinone/plastoquinol exchange between the inter-monomer cavity and bilayer (2Fo-Fc electron density map contoured at σ=1.0 (~0.1 electrons/Å^3). The acidic sulfolipid molecule of cyt b_6f interacts with Lys275 (cyt *f*) and Arg16 and Asn20 (ISP). **(B)** The sulfolipid (wheat, transparent) is located close to the acidic PA (green) and detergent UDM (teal) of the bc_1 complex suggesting an important role for this lipid binding niche.
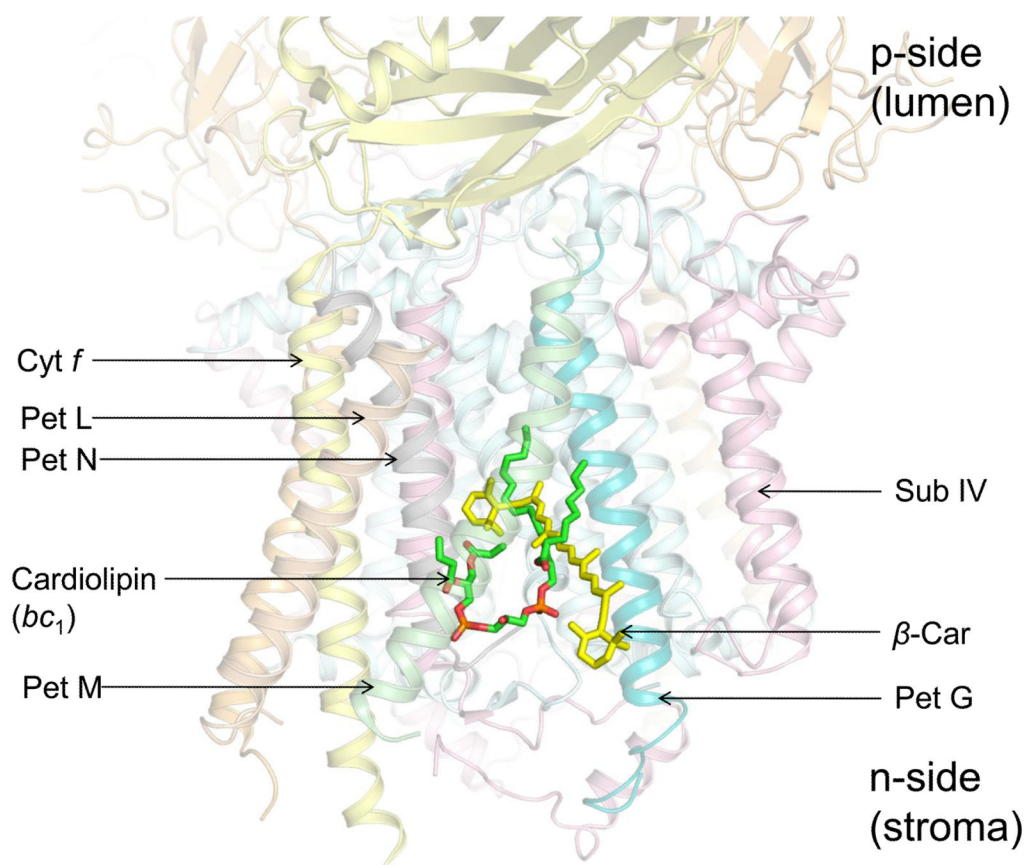
Fig 7. Super-complex formation; bridge to photosystem I

Cardiolipin of cyt bc_1 (green and red) is involved in stabilizing super-complexes with cyt c oxidase (55). Superposition of the bc_1 complex (PDB ID 3CX5) with the cyanobacterial b_6f complex (PDB ID 2E74) results in close spatial location of cardiolipin (acyl chains, green; orange and red are head group phosphorous and oxygen atoms respectively) and $β$–carotene (yellow), which has been suggested to mediate a cyt b_6f-PSI supercomplex (5).
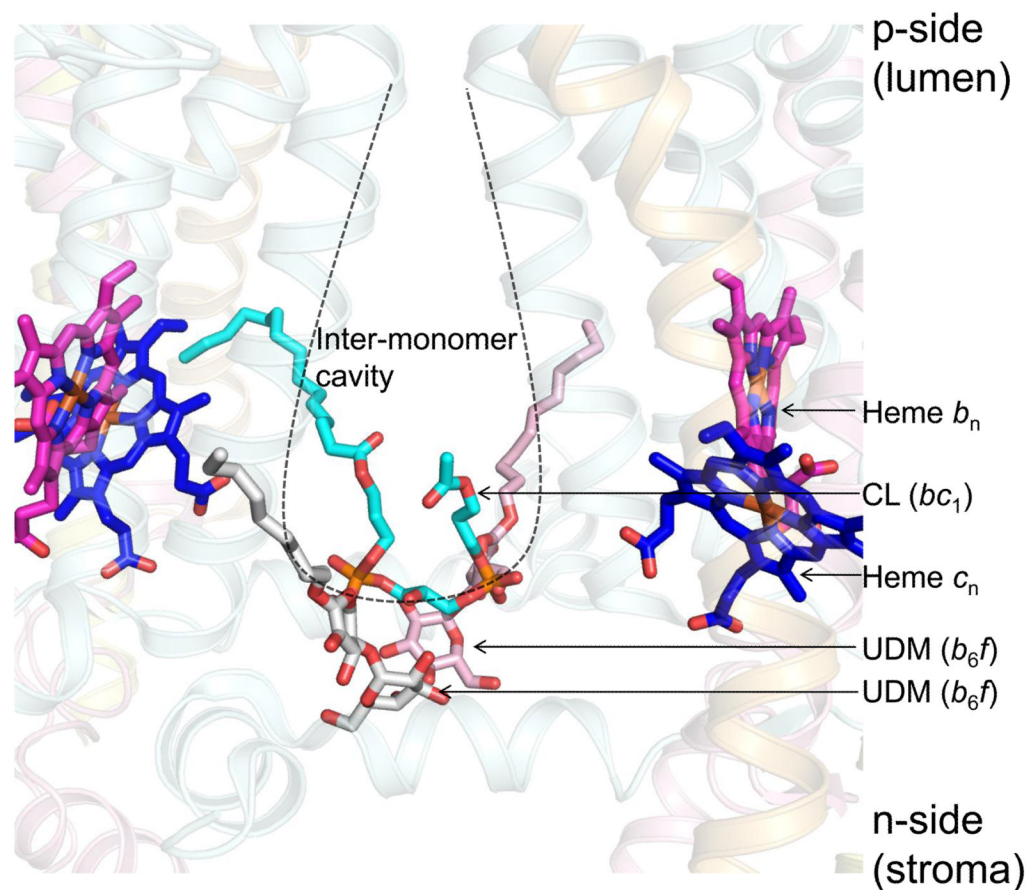
Fig 8. *n*-side H$^+$ antenna function
An acidic cardiolipin molecule (cyan), shared between the two monomers of the bc_1 complex (PDB ID 3CX5). Two detergent molecules (white/red and pink/red, one from each monomer) are found in the same position in the cyanobacterial cyt b_6f complex (*M. laminosus*, PDB ID 2E74) when the structures are superposed and may mark the position of a lipid molecule.

Table 1

Summary of structural superposition of cytochrome *bc* complexes (details described in methods section)

Cyt $b_6 f$	Cyt bc_1	Superposition method	Cα RMSD (Å)
2E74 (Chain B, Asn34-Phe160)	3CX5 (Chain C, Lys228-Ile354)	Cα-based pair-fitting	4.70
2E74, 1Q90	--	Global alignment	0.65
2E74	3CX5	Global alignment	1.29

Table 2

B-factor summary of cyt b_6f polypeptides (PDB ID 2E74)

Subunit	Residue B-factor (Å²)	Backbone B-factor (Å²)
Cyt b_6 (A)	45	45
Sub IV (B)	62	61
Cyt f (C)[*]	64 (TMH:48, SD: 65)	64 (TMH:48, SD:65)
ISP (D)[**]	91 (TMH:53, SD:97)	92 (TMH:52, SD:98)
Pet L (E)	81	80
Pet M (F)	76	73
Pet G (G)	71	69
Pet N (H)	58	57

[*] Cyt f (chain C): TMH (trans-membrane helix) residues 255–274; SD (soluble domain) residues 1–254 and 275–289

[**] ISP (chain D): TMH residues 17–39; SD residues 9–16 and 40–179; Chain IDs A-H for PDB ID 2E74 mentioned in parentheses.

Table 3

B-factor analysis of lipids and detergents in cyt b_6f (PDB ID 2E74)[&], [&&]

Ligand	Ligand B- factor (average, Å^2)	Head group B-factor (average, Å^2)	Tail B-factor (average, Å^2)	Binding site B-factor (average, Å^2)	Binding site backbone B-factor (average, Å^2)
SQD (D201)	107	107	--	56	55
DOPC$_p$ (H1002)	100	164	77	60	56
DOPC$_n$ (B202)	80	80	79	62	62
UDM$_p$ (A1101)	101	122	52	42	41
UDM$_{n1}$ (A1102)	113	132	76	58	59
UDM$_{n2}$ (A1104)	126	136	91	67	66
UDM$_{n3}$ (A1103)	111	115	87	72	67

[&] 2Fo-Fc map contoured at 1.0 sigma (~0.1 electrons/Å^3) in COOT. Ligand and amino acid atoms within electron density envelope included in analysis.

[&&] Details of lipids, detergents and binding site residues in Supplementary material, Tables S2a–g and S6.